S-MATRIX DESCRIPTION OF REFRACTIVE EFFECTS IN ONE-NUCLEON STRIPPING REACTIONS INDUCED BY α-PARTICLES ON ^{28}Si

Yu.A. Berezhnoy[a], A.S. Molev[a,b]

[a]Karazin Kharkov National University, Kharkov 61022, Ukraine
[b]Institute of Electrophysics and Radiation Technologies, Kharkov 61002, Ukraine

Received 15 July 2021, accepted 5 January 2022, published online 11 February 2022

We analyze the angular distributions for the (α, ^{3}He) and (α, t) reactions on ^{28}Si for projectile energies ranging from 50 to 120 MeV based on the partial-wave representation of the transfer amplitude expressed in terms of the S-matrices for the entrance and exit channels, with an emphasis on identifying Airy minima of various orders. The calculations have been performed using a six-parameter S-matrix model and S-matrix parameters obtained from the analysis of elastic scattering data. The first- and (or) second-order Airy minima are clearly identified in the analyzed transfer reaction angular distributions at intermediate angles. The detected Airy minima are found to be due to the interference between several inner and surface partial waves. The impact parameters of these waves are in the range of 1–6 fm, the upper boundary of which is less than the strong absorption radius.

DOI:10.5506/APhysPolB.53.2-A1

1. Introduction

In α+^{28}Si elastic and inelastic scattering at projectile energies of $E = 50$–120 MeV, various refractive effects are observed, such as a nuclear rainbow and Airy minima of the first ($A1$) and (or) second ($A2$) orders, which are a key ingredient in the unambiguous determination of the characteristics of the nucleus–nucleus interaction (see, *e.g.*, Refs. [1, 2]). These refractive effects were revealed [3] as a result of a systematic data analysis within the S-matrix formalism using a six-parameter S-matrix model [4].

In this context, it seems important using these results for α+^{28}Si scattering to perform an S-matrix analysis of the one-nucleon transfer reactions induced by α-particles and to find out whether the indicated refractive effects are manifested in these reactions. The appearance of such effects depends on the correspondence between a number of parameters of the entrance and

exit channels (see, *e.g.*, Refs. [5, 6]). The procedure for identifying Airy minima in transfer reaction angular distributions is similar to that used in the case of elastic scattering (*e.g.*, Refs. [3, 7, 8]).

To perform S-matrix analysis of the one-nucleon transfer reactions, we use the partial-wave representation of the transfer amplitude [9, 10] expressed in terms of the S-matrices for the entrance and exit reaction channels. In this case, the Hahne representation [11] of the transition matrix element is applied, which is an extension of that of Austern–Blair [12] for inelastic scattering. In this approach, it is assumed that the Hahne representation of the transition matrix element for inelastic scattering is also applicable to transfer reactions populating the levels of the final nuclei by a one-step process. Of course, the consequence of the applied simplifications is the loss of the spectroscopic strength but, at the same time, the dynamics of the transfer reaction, Q-value dependence, and transfer angular momentum matching are properly described (for more details see, *e.g.*, Refs. [9, 10, 13]).

Parametrization [4] was taken as S-matrices for the entrance and exit channels since it turned out to be very successful in describing the nuclear rainbow pattern and refractive patterns with Airy minima (see, *e.g.*, Refs. [3, 14]). The S-matrix parameters have been derived from the analysis of the elastic scattering data for both entrance and exit channels.

Within this approach, Airy minima $A1$ and $A2$ have been identified for the first time in the differential cross sections for the ^{28}Si(α, ^{3}He)^{29}Si and ^{28}Si(α, t)^{29}P reactions with the transition to the ground states of the final nuclei at $E_\alpha = 50$–120 MeV. The formation of these minima due to particular partial waves has been analysed.

2. Results of calculations

We have performed calculations of the angular distributions for the ^{28}Si(α, ^{3}He)^{29}Si reaction with the $\ell = 0$ (here, ℓ is the transfer angular momentum) transition to the ground state ($1/2^+$) in ^{29}Si (Q-value of reaction is -12.104 MeV) at $E_\alpha = 64.9$ and 120.0 MeV, and for the ^{28}Si(α, t)^{29}P reaction with the $\ell = 0$ transition to the ground state ($1/2^+$) in ^{29}P ($Q = -17.065$ MeV) at $E_\alpha = 50.0$ and 64.9 MeV. Note that the indicated transfer momentum was defined in Ref. [15].

For a transfer reaction with a zero transfer momentum involving spinless nuclei and neglecting the nuclear recoil effect, the differential cross section within the framework of the distorted-wave Born approximation is given by [9]

$$\frac{\mathrm{d}\sigma}{\mathrm{d}\Omega}(\theta) = \frac{m_\mathrm{i} m_\mathrm{f}}{(2\pi\hbar^2)^2}\frac{k_\mathrm{f}}{k_\mathrm{i}}|T(\theta)|^2 , \qquad (1)$$

$$T(\theta) = \tau \frac{\sqrt{4\pi}}{k_{\rm i} k_{\rm f}} \sum_{l=0}^{\infty} (2l+1) e^{i\left(\sigma_l^{\rm i} + \sigma_l^{\rm f}\right)} \beta_l P_l(\cos\theta)\,, \tag{2}$$

where θ is the scattering angle, the indices 'i' and 'f' refer to the entrance and exit channels, respectively, m is the reduced mass, k is the wave number of relative motion, τ is the transfer parameter, σ_l is the Coulomb scattering phase, and β_l is the transition matrix element.

The transition matrix element is taken in the form of [11]

$$\beta_l = \frac{1}{2i} \left[E_{\rm cm}^{\rm i} E_{\rm cm}^{\rm f} \frac{\partial S_l^{\rm i}}{\partial l} \frac{\partial S_l^{\rm f}}{\partial l} \right]^{1/2}, \tag{3}$$

where $E_{\rm cm}^{\rm i(f)}$ is the center-of-mass energy in the entrance (i) or exit (f) channel, $S_l^{\rm i}$ and $S_l^{\rm f}$ are the nuclear S-matrix elements in the state with angular momentum l in the entrance and exit channels, respectively. The applicability of expression (3) to the considered transfer reactions was discussed in the introduction. The use of (3) makes it possible to perform calculations directly in the angular momentum space if the representations of the S-matrix elements $S_l^{\rm i}$ and $S_l^{\rm f}$ are chosen.

In our analysis of $(\alpha,\ ^3{\rm He})$ and $(\alpha,\ t)$ reactions on ^{28}Si, the nuclear S-matrix element as a complex function of the angular momentum $L = l+1/2$ both in the entrance and exit channels has the following parameterized form [4]:

$$S(L) = \eta(L) \exp\left[2i\delta_{\rm r}(L)\right], \quad \eta(L) = \exp\left[-2\delta_0 g(L, L_0, \Delta_0)\right], \tag{4}$$

$$\delta_{\rm r}(L) = \delta_1 g^2(L, L_1, \Delta_1)\,, \tag{5}$$

$$g(L, L_j, \Delta_j) = \frac{\sinh\left(\frac{L_j}{\Delta_j}\right)}{\cosh\left(\frac{L_j}{\Delta_j}\right) + \cosh\left(\frac{L}{\Delta_j}\right)}, \quad j = 0, 1\,, \tag{6}$$

where $\eta(L)$ is the scattering matrix modulus, $\delta_{\rm r}(L)$ is the nuclear refraction phase, the parameters $2\delta_{0,1}$ are measures of the intensity of absorption and nuclear refraction, respectively, L_j and Δ_j are the parameters, characterizing the size and diffuseness of the absorption ($j = 0$) and refraction ($j = 1$) regions, the indices 'i' and 'f' indicating the entrance and exit channels are omitted for all presented quantities and parameters. It is convenient to introduce the relation $2\delta_0 = -\ln\varepsilon$, where ε is the nuclear transparency.

The characteristic features of the one-nucleon stripping reaction cross sections are analyzed using the nearside–farside decomposition [16], which is applicable in the usual way due to the presence of the Legendre polynomials in (2). To detect Airy minima, we study the behavior of both the farside

component of transfer reaction cross section under consideration and the farside cross-section component obtained in the case of turned-off absorption in the entrance channel (see, *e.g.*, Refs. [17, 18]). In the latter case, when calculating (3), we set $|\ S_l^{\rm i}\ | = 1$ for all l. The minimum of the cross section, which is described by the farside cross-section component and whose angular position is the same or close enough to that for the Airy minimum of a particular order in the farside component, calculated with the turned-off absorption in the entrance channel, is identified as the Airy minimum of the same particular order.

At the first stage of our work, the S-matrix parameters for the entrance channel of the studied (α, ^{3}He) and (α, t) reactions on ^{28}Si are derived from the analysis of the α+^{28}Si elastic scattering data at energies under consideration. The parameters at $E_\alpha = 50.0$ and 120.0 MeV (see Table 1) were taken from Ref. [3], and at $E_\alpha = 64.9$ MeV were obtained from the agreement of the calculated cross section both with the result of the optical model analysis of the data (unpublished) at the same energy (see Ref. [15]) and with the existing data for the neighboring system α+^{27}Al at 64.5 MeV (see Fig. 1). The calculations were performed using the elastic scattering amplitude in the form of a standard expansion into a series of Legendre polynomials. The nuclear part of the S-matrix had the representation of (4)–(6), and the Coulomb scattering phase was taken in the form of [3, 4]. The obtained S-matrix parameters for 64.9 MeV are listed in Table 1.

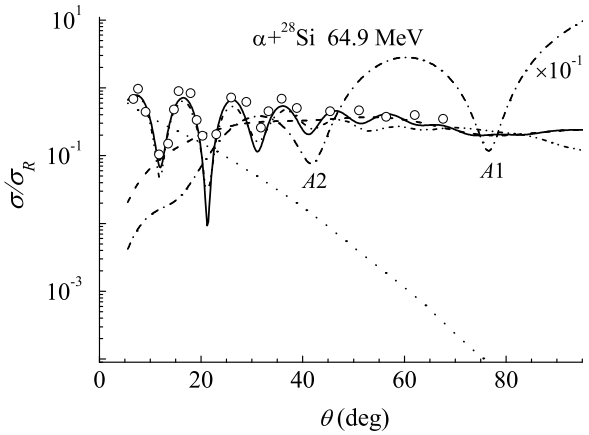

Fig. 1. The calculated differential cross section (normalized to the Rutherford cross section) for the α+^{28}Si elastic scattering at $E_\alpha = 64.9$ MeV (solid curve), its farside (dashed curve) and nearside (dotted curve) components, and the farside cross-section component calculated with the turned-off absorption (dash-dotted curve). The dash-double-dotted curve shows the results [15] for the optical model calculations. Aν is the $\nu^{\rm th}$ order of the Airy minimum. The data are from Ref. [19].

Table 1. S-matrix parameters for the α+^{28}Si elastic scattering used as the entrance channel parameters.

E_α [MeV]	L_0	L_1	Δ_0	Δ_1	ε	$2\delta_1$	Ref.
50.0	13.102	11.197	1.781	2.888	0.00752	30.150	[3]
64.9	14.761	12.850	1.970	3.243	0.01500	27.298	this work
120.0	19.587	17.048	2.855	5.070	0.03800	19.628	[3]

The next stage of the work is associated with finding the S-matrix parameters for the exit channels of the transfer reactions under consideration. Due to the non-availability of data on the ^{3}He+^{29}Si and t+^{29}P elastic scattering at the required energies, we will obtain the exit channel parameters from the results of the analysis of the available data for systems adjacent to the indicated ones at close to the required energies. Thus, as the S-matrix parameters for the exit channel of the ^{28}Si(α, ^{3}He)^{29}Si reaction at $E_\alpha = 64.9$ and 120.0 MeV we will use the parameters obtained from the description of the elastic scattering angular distributions for ^{3}He+^{28}Si at 60.0 MeV and ^{3}He+^{27}Al at 119.0 MeV, respectively. The S-matrix parameters for the exit channel of the ^{28}Si(α, t)^{29}P reaction at $E_\alpha = 50.0$ and 64.9 MeV will be the parameters producing the best fits to the elastic scattering angular distributions for t+^{30}Si at 36.0 MeV and ^{3}He+^{29}Si at 46.0 MeV, respectively. The results of the elastic scattering data analysis for the systems listed above using the parametrization of (4)–(6) are shown in Fig. 2. The spin–orbit part of the nuclear S-matrix was not taken into account in the calculations due to its unimportant effect on the scattering cross section (*e.g.*, Refs. [17, 20]). The quality of fitting the experimental data was determined by means of the usual χ^2/N (N is the number of data points) magnitude. A uniform uncertainty of 10% was assumed for all considered experimental cross-section points. The calculation parameters and the values of χ^2/N are given in Table 2.

Table 2. S-matrix parameters for elastic scattering of various systems used as the exit channels parameters.

System	E_α [MeV]	L_0	L_1	Δ_0	Δ_1	ε	$2\delta_1$	χ^2/N
t+^{30}Si	36.0	9.344	6.482	1.684	2.815	0.00746	28.945	15.9
^{3}He+^{29}Si	46.0	11.557	8.247	1.667	2.494	0.02320	22.437	9.9
^{3}He+^{28}Si	60.0	12.163	9.564	2.330	3.408	0.01484	22.204	9.7
^{3}He+^{27}Al	119.0	17.088	15.191	2.614	4.459	0.04064	14.289	3.2

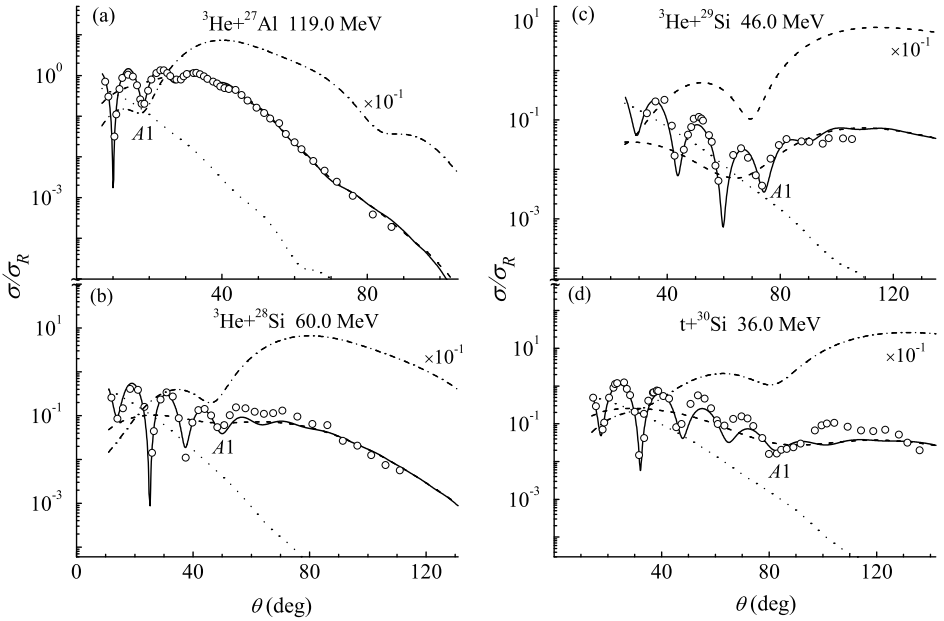

Fig. 2. The same as in Fig. 1, but for the ^{3}He+^{27}Al at 119.0 MeV (a), ^{3}He+^{28}Si at 60.0 MeV (b), ^{3}He+^{29}Si at 46.0 MeV (c), and t+^{30}Si at 36.0 MeV (d). The data are from Refs. [20–23].

Using (1)–(6) and parameters for $S^{\rm i}(L)$ from Table 1 and for $S^{\rm f}(L)$ from Table 2, we have calculated the differential cross sections for the ^{28}Si(α, ^{3}He)^{29}Si, and ^{28}Si(α, t)^{29}P reactions accompanied by the transition to the ground states of final nuclei within the incident energy range 50–120 MeV (dash-double-dotted curve in Fig. 3 (a), (b), (c), and (d), obtained with $\tau = 0.328$, 0.341, 0.300 and 0.211 fm, respectively). We have also obtained the farside components of these cross sections for the case of turned-off absorption in the entrance channel (short-dashed curves in Figs. 3 (a)–(d)). Note that the description of the cross sections for the indicated one-nucleon stripping reactions is performed without using any fitting S-matrix parameters for both reaction channels and serves as a critical test for the results of the analysis of the elastic scattering cross sections.

When refining the parameter values for the exit channels of the considered transfer reactions, based on the corresponding values of Table 2, a slight variation of the latter (mainly within 10%) seems legitimate for better agreement between the calculation results and the data. Differential cross sections calculated with the exit channel parameters changed in this way (see Table 3, parameter τ for each reaction was not varied) and the

entrance channel parameters of Table 1 are displayed in Fig. 3 together with their nearside–farside components. Table 3 also shows the values of $\chi^2_{\rm tr}/N$ (10% error bars) for the calculated cross sections.

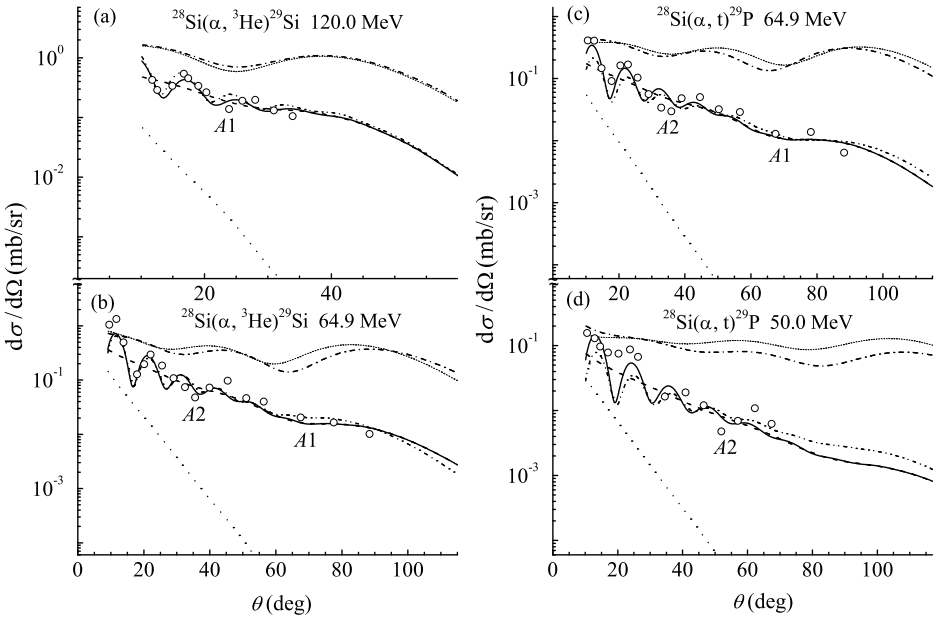

Fig. 3. (a) The differential cross section for the ^{28}Si(α, ^{3}He)^{29}Si reaction populating the ground state of ^{29}Si (solid curve) at $E_\alpha = 120.0$ MeV, calculated using parameters of Tables 1 and 3, its farside (dashed curve) and nearside (dotted curve) components, and the farside cross-section component obtained with the turned-off absorption in the entrance channel (dash-dotted curve). The dash-double-dotted and short-dashed curves display the results of the calculations with the parameters of Tables 1 and 2 (see the text). (b) The same as in (a), but for $E_\alpha = 64.9$ MeV. (c) and (d) The same as in (a), but for the ^{28}Si(α, t)^{29}P reaction populating the ground state of ^{29}P at $E_\alpha = 64.9$ and 50.0 MeV, respectively. Aν is the $\nu^{\rm th}$ order Airy minimum. The experimental data are from Ref. [15].

From Fig. 3 we see that the results of both versions of calculating the transfer reaction cross sections are mostly close to each other in the measured angular range, which makes it possible to use them equally for revealing Airy structures. In general, the agreement between the calculated and measured transfer reaction cross sections is reasonable in view of the simplifying assumptions (see Refs. [10, 11]) made to obtain (2) and (3).

Table 3. Exit channel parameters used in calculating the transfer reaction cross sections and the χ^2 magnitude per datum.

Reaction	(α, t)	(α, t)	$(\alpha, {}^3\mathrm{He})$	$(\alpha, {}^3\mathrm{He})$
E_α [MeV]	50.0	64.9	64.9	120.0
L_0^f	10.200	12.027	12.960	15.704
L_1^f	6.638	8.513	9.982	13.636
Δ_0^f	1.991	2.016	2.346	2.317
Δ_1^f	2.690	2.742	3.286	4.361
ε^f	0.00673	0.02181	0.01510	0.03862
$2\delta_1^\mathrm{f}$	29.011	21.872	23.107	14.733
τ [fm]	0.211	0.300	0.341	0.328
χ^2_tr/N	17.9	13.2	10.9	3.6

3. Interpretation of the calculation results in terms of Airy minima

The ^{28}Si$(\alpha, {}^3\mathrm{He})^{29}$Si reaction leading to the ground state of ^{29}Si at $E_\alpha =$ 120.0 MeV refers to the case when a nuclear rainbow is observed in elastic scattering of nuclei interacting in both the entrance and exit channels (see Ref. [3] and Fig. 2 (a)). As can be seen in Fig. 3 (a), the differential cross section for this reaction also displays a pattern characteristic of a nuclear rainbow preceded by the Airy minimum $A1$, which turns out to be shifted towards smaller angles compared with that for the α+^{28}Si elastic scattering (see Fig. 4).

Considering the $(\alpha, {}^3\mathrm{He})$ and (α, t) reactions on ^{28}Si at $E_\alpha = 64.9$ and 50.0 MeV, we are dealing with the case when the pattern of elastic scattering of nuclei interacting in the entrance channel (refractive pattern with minima $A1$ and $A2$ (see Fig. 1 and Ref. [3])) and that in the exit channel (nuclear rainbow/prerainbow pattern only with $A1$ (see Figs. 2 (b)–(d))) are quite different. The calculated angular distributions for the ^{28}Si$(\alpha, {}^3\mathrm{He})^{29}$Si and ^{28}Si$(\alpha, t)^{29}$P reactions at $E_\alpha = 64.9$ MeV are characterized by a well-marked $A2$ minimum and a weakly pronounced $A1$ minimum (see Figs. 3 (b) and (c)), whereas in the available data for each of these reactions one can notice only a hint of $A1$ minimum. Figure 3 (d) indicates that a weakly pronounced $A2$ minimum is retained in the differential cross section for the ^{28}Si$(\alpha, t)^{29}$P reaction at $E_\alpha = 50.0$ MeV, being at a position shifted forward from that in the case of α+^{28}Si elastic scattering (see Fig. 4), but the $A1$ minimum disappears.

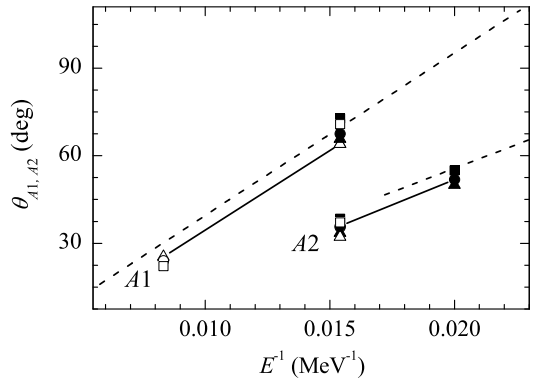

Fig. 4. Dependence on the inverse energy of the angular positions of the Airy minima $A1$ and $A2$ in the calculated differential cross sections for the ^{28}Si(α, ^{3}He)^{29}Si (open squares) and ^{28}Si(α, t)^{29}P (solid squares) reactions and in their farside components obtained with the turned-off absorption in the entrance channel (open and solid triangles for the ^{28}Si(α, ^{3}He)^{29}Si and ^{28}Si(α, t)^{29}P reactions, respectively), and in the measured data (open and solid circles for the ^{28}Si(α, ^{3}He)^{29}Si and ^{28}Si(α, t)^{29}P reactions, respectively). Both the open triangles for $A1$ and the solid circles for $A2$ are connected by solid lines. The dashed lines for $A1$ and $A2$, related to the α+^{28}Si elastic scattering, are taken from Ref. [3] and shown for comparison.

Let us find out which particular partial waves are responsible for the appearance of the identified Airy minima in the calculated cross sections for the (α, ^{3}He) and (α, t) reactions on ^{28}Si. To do this, we split the transition amplitude (2) into the sum of three subamplitudes for the ranges $\Delta l_1 = 0 \div l_m - 1$, $\Delta l_2 = l_m \div l_n$, and $\Delta l_3 = l_n + 1 \div \infty$. The angular momenta l_m and l_n are determined proceeding from the fact that we are looking for the narrowest possible Δl_2, for which the calculated component of the transfer reaction cross section continues to describe all available Airy minima and their surroundings. The cross-section components calculated for Δl_2 and Δl_3 have little effect on the formation of the mentioned Airy minima.

Figure 5 presents our results obtained in such a way: we found $\Delta l_2 = 6 \div 23$ (corresponding impact parameter range $\Delta b_2 = \Delta l_2/k_{\rm i} = 1.4 \div 5.5$ fm) for the ^{28}Si(α, ^{3}He)^{29}Si reaction at $E_\alpha = 120.0$ MeV, $\Delta l_2 = 2 \div 16$ and $3 \div 18$ ($\Delta b_2 = 0.7 \div 5.9$ and $1.0 \div 5.8$ fm) for the ^{28}Si(α, t)^{29}P reaction at E_α= 50.0 and 64.9 MeV, respectively (the boundaries of the ranges Δl_1 and Δl_3 adjacent to Δl_2 on both sides are obvious). The dashed, dash-double-dotted, and dotted curves are calculated for Δl_2, Δl_3 and Δl_1, respectively.

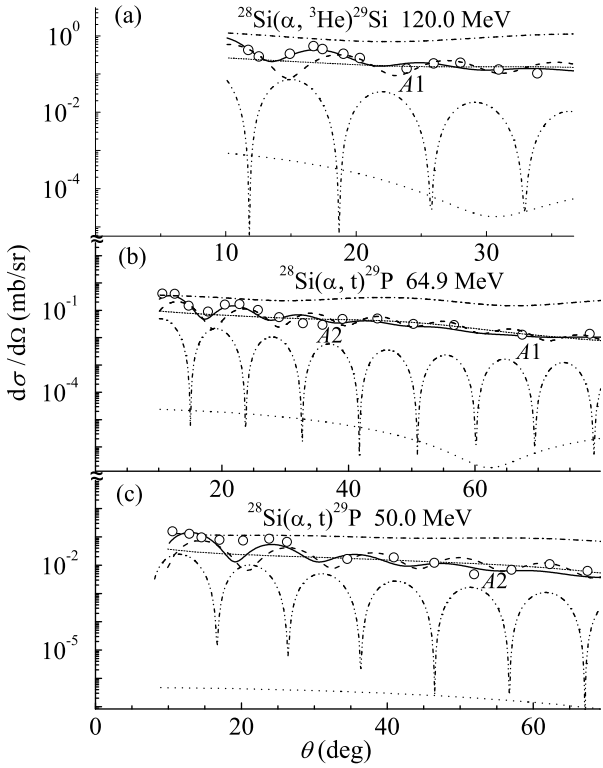

Fig. 5. Analysis of formation of Airy minima in the differential cross sections for the ^{28}Si(α, ^{3}He)^{29}Si and ^{28}Si(α, t)^{29}P reactions leading to the ground states of the final nuclei at E_α = 50–120 MeV. (a) The solid curve and the data are the same as in Fig. 3 (a). The cross-section components obtained for the found range $\Delta l_2 = 6 \div 23$ and for the ranges Δl_1 and Δl_3, adjacent to Δl_2 on both sides ($l < 6$ and $l > 23$), are shown by the dashed, dotted, and dash-double-dotted curves, respectively. The short-dashed and dash-dotted curves represent the farside contributions to the cross-section component shown by the dashed curve (see the text). (b) The same, as in (a), but for the ^{28}Si(α, t)^{29}P reaction at $E_\alpha = 64.9$ MeV. The solid curve and the data are the same as in Fig. 3 (c) and $\Delta l_2 = 3 \div 18$. (c) The same, as in (a), but for the ^{28}Si(α, t)^{29}P reaction at $E_\alpha = 50.0$ MeV. The solid curve and the data are the same as in Fig. 3 (d) and $\Delta l_2 = 2 \div 16$.

From Fig. 5 we see that in each of the considered cases the cross-section component obtained for Δl_2 (dashed curve) represents the major contribution to the corresponding total cross section (solid curve) in the measured angular range. This component is farside dominated (as shown by the short-dashed curve). The farside contribution to the considered cross-section component in the case of turned-off absorption in the entrance channel (dash-

dotted curve) is characterized by the presence of $A1$ and (or) $A2$ minima at angles close to those for the Airy minima in the experimental data. The cross-section components obtained for Δl_1 and Δl_3 are small.

Consider the localization of the found Δl_2 ranges in l-space. To be specific, surface waves are considered to be those that have angular momenta for which $\mid S_l^{\mathrm{i}} \mid$ varies from 0.1 to 0.9 (see Ref. [24]), and inner waves are those for which $\mid S_l^{\mathrm{i}} \mid < 0.1$. Then, each of the indicated Δl_2 ranges includes several inner waves with momenta up to $l = 16$, 13, and 12 for the cases shown in Figs. 5 (a), (b) and (c), respectively. The rest of the waves related to Δl_2 are surface waves. They have momenta less than the strong absorption momentum $l_{\mathrm{sa}}^{\mathrm{i}} = 25.18$, 19.01 and 17.16 (corresponding strong absorption radius $R_{\mathrm{sa}}^{\mathrm{i}} = 6.29$, 6.67 and 6.98 fm) for the cases shown in Figs. 5 (a), (b) and (c), respectively.

This indicates that such a refractive effect in the one-nucleon stripping reactions induced by α-particles on ^{28}Si as the first(second)-order Airy minimum is due to the interference between several inner and surface waves. The impact parameters of these partial waves fall within the range, the upper boundary of which is less than the strong absorption radius.

4. Conclusion

Using the partial-wave representation of the transfer amplitude expressed in terms of the S-matrices for the entrance and exit reaction channels, we have analyzed the angular distributions for the (α, ^{3}He) and (α, t) reactions on ^{28}Si populating the ground states of the final nuclei at $E_\alpha = 50$–120 MeV, focusing on the detection of Airy minima of various orders. We have used a six-parameter S-matrix model [4] and S-matrix parameters obtained from the analysis of available elastic scattering data for the system in the entrance channel and for the systems adjacent to those in the exit channels.

We have clearly identified a nuclear rainbow with a preceding $A1$ minimum in the differential cross section for ^{28}Si(α, ^{3}He)^{29}Si at $E_\alpha = 120.0$ MeV, $A1$ and $A2$ minima in the cross sections for ^{28}Si(α, ^{3}He)^{29}Si and ^{28}Si(α, t)^{29}P at $E_\alpha = 64.9$ MeV, and only $A2$ minimum in the cross section for ^{28}Si(α, t)^{29}P at $E_\alpha = 50.0$ MeV.

The identified $A1$ and $A2$ minima are formed due to the interference between several inner and surface partial waves. The impact parameters of these partial waves are in the range from 1 to 6 fm, whereas the strong absorption radius is somewhat greater than 6 fm. This indicates to what extent the studied transfer reaction cross sections containing Airy minima are sensitive to the interaction in the nuclear interior.

REFERENCES

[1] D.T. Khoa, W. von Oertzen, H.G. Bohlen, S. Ohkubo, «Nuclear rainbow scattering and nucleus–nucleus potential», *J. Phys. G: Nucl. Part. Phys.* **34**, R111 (2007).

[2] M.E. Brandan, M.S. Hussein, K.W. McVoy, G.R. Satchler, «Airy's Pot of Gold: What Rainbows Are Teaching Us About Nuclear Scattering», *Comments Nucl. Part. Phys.* **22**, 77 (1996).

[3] Yu.A. Berezhnoy, A.S. Molev, «Airy minima in ^{4}He+^{28}Si elastic and inelastic scattering», *Mod. Phys. Lett. A* **35**, 2050159 (2020).

[4] Yu.A. Berezhnoy, V.V. Pilipenko, «Analysis of Refraction Effects in Nuclear Scattering on the Basis of the S-matrix Approach», *Mod. Phys. Lett. A* **10**, 2305 (1995).

[5] A.S. Demyanova *et al.*, «Rainbow effects in charge exchange reactions», *Nucl. Phys. A* **482**, 383 (1988).

[6] H.G. Bohlen *et al.*, «One-neutron transfer reaction and refractive effects in the ^{16}O+^{16}O system», *Nucl. Phys. A* **703**, 573 (2002).

[7] Yu.A. Glukhov *et al.*, «Nuclear rainbow in the elastic scattering of ^{16}O nuclei on carbon isotopes», *Phys. Atom. Nuclei* **70**, 1 (2007).

[8] V.Yu. Korda, A.S. Molev, V.F. Klepikov, L.P. Korda, «Unified model-independent S-matrix description of nuclear rainbow, prerainbow, and anomalous large-angle scattering in ^{4}He–^{40}Ca elastic scattering», *Phys. Rev. C* **91**, 024619 (2015).

[9] M.C. Mermaz, «Regge-pole analysis of angular distribution for the ^{24}Mg(^{16}O, ^{12}C)^{28}Si reaction», *Phys. Rev. C* **24**, 773 (1981).

[10] M.C. Mermaz, «Several applications of the DWBA diffractional model of quasi-elastic reactions induced by heavy ions», *Nuovo Cim. A* **81**, 291 (1984).

[11] F.J.W. Hahne, «A modification of the Austern–Blair theory and the study of $(\alpha, \alpha'\gamma)$ correlation functions», *Nucl. Phys. A* **104**, 545 (1967).

[12] N. Austern, J.S. Blair, «Calculation of inelastic scattering in terms of elastic scattering», *Ann. Phys.* **33**, 15 (1965).

[13] R.I. Badran, I.M. Naqib, D.J. Parker, J. Asher, «Strong absorption formalism applied to the direct transfer reaction ^{56}Fe(^{7}Li, ^{4}He)^{59}Co* leading to continuum states», *J. Phys. G: Nucl. Part. Phys.* **22**, 1441 (1996).

[14] Yu.A. Berezhnoy, A.S. Molev, G.M. Onyshchenko, V.V. Pilipenko, «Unified S-matrix analysis of Airy structures in α+^{24}Mg elastic and inelastic scattering», *Int. J. Mod. Phys. E* **27**, 1850061 (2018).

[15] V.P. Darshan *et al.*, «Study of $(\alpha, {}^{3}\mathrm{He})$ and (α, t) reactions on ^{28}Si at 45 MeV», *J. Phys. G: Nucl. Part. Phys.* **21**, 385 (1995).

[16] R.C. Fuller, «Qualitative behavior of heavy-ion elastic scattering angular distributions», *Phys. Rev. C* **12**, 1561 (1975).

[17] V. Burjan *et al.*, «Rainbowlike effects in$({}^{3}\mathrm{He}, \alpha)$ reactions», *Phys. Rev. C* **49**, 977 (1994).

[18] A.S. Dem'yanova *et al.*, «Rainbows in nuclear reactions and the optical potential», *Phys. Scr.* **T32**, 89 (1990).

[19] M. Yasue *et al.*, «Excitation of high-spin particle-hole states in $A = 28$ nuclei by ^{27}Al(α, t) and (α, ^{3}He) reactions», *Nucl. Phys. A* **391**, 377 (1982).

[20] M. Hyakutake *et al.*, «Elastic scattering of 119 MeV ^{3}He particles and energy and mass-number dependence of optical potential parameters», *Nucl. Phys. A* **333**, 1 (1980).

[21] K.B. Basybekov, N. Burtebaev, A. Duisebaev, «Scattering of 60 MeV ^{3}He ions by 1d–2s shell nuclei», *Izv. Minister. Nauki Akad. Nauk Resp. Kaz. Ser. Fiz.-Mat.* **6**, 28 (1998).

[22] C.B. Fulmer *et al.*, «Scattering of 41-MeV α particles and 46-MeV ^{3}He from ^{27}Al, ^{28}Si, ^{29}Si, and ^{30}Si», *Phys. Rev. C* **18**, 621 (1978).

[23] K.I. Pearce *et al.*, «36 MeV triton inelastic scattering and one-nucleon transfer reactions», *Nucl. Phys. A* **467**, 215 (1987).

[24] I. Jamir, E.F.P. Lyngdoh, C.S. Shastry, «α-nucleus scattering in angular momentum space», *Phys. Rev. C* **57**, 1000 (1998).